Self-aligned dual-beam optical laser trap using photorefractive phase conjugation

W. Wang

Department of Electrical and Computer Engineering and Beckman Laser Institute and Medical Clinic, University of California, Irvine, Irvine, California 92697

A. E. Chiou

Rockwell International Science Center, 1049 Camino Dos Rios, Thousand Oaks, California 91360

G. J. Sonek

Department of Electrical and Computer Engineering and Beckman Laser Institute and Medical Clinic, University of California, Irvine, Irvine, California 92697

M. W. Berns

Beckman Laser Institute and Medical Clinic, University of California, Irvine, Irvine, California 92697

Received May 20, 1996; revised manuscript received August 26, 1996

We report what is to our knowledge the first experimental demonstration and theoretical analysis of an optical laser trap that uses a pair of mutually phase-conjugate beams. A primary trapping beam derived from an argon laser (514.5 nm) together with its counterpropagating phase-conjugate beam creates a self-aligned dual-beam laser trap that provides stable three-dimensional confinement for micrometer-sized dielectric particles. The transverse trapping efficiency, experimentally measured for low-numerical-aperture (N.A. 0.40–0.85) objective lenses, is found to be comparable with that produced by a single-beam gradient force trap. A theoretical analysis, which compares the performance of the self-aligned dual-beam trap against that of single-beam gradient force and conventional counterpropagating dual-beam laser traps, shows that phase-conjugate trapping provides a slight improvement in axial trapping efficiency over the other trapping geometries. The advantages of combining laser trapping with photorefractive optical phase conjugation for simultaneous sample micromanipulation and optical image processing are discussed. © 1997 Optical Society of America [S0740-3224(97)00804-7]

1. INTRODUCTION

In 1969 Ashkin demonstrated that two counterpropagating mildly focused laser beams form a stable three-dimensional trap for small dielectric spheres[1] [Fig. 1(a)]. Later, in 1985, a stable single-beam gradient force optical trap[2] [Fig. 1(b)] was successfully demonstrated. Since then, optical laser traps in both dual-beam and single-beam geometries have been developed and used extensively for sample micromanipulation and force transduction.[3,4] Recently a self-aligned dual-beam laser trap [Fig. 1(c)] was proposed[5] that integrates, in a common system, the technologies of laser trapping and photorefractive optical phase conjugation for sample micromanipulation and optical image processing. In optical phase conjugation (OPC),[6] a nonlinear medium and an input laser beam are used to generate a reflected (phase-conjugate) beam that precisely reverses the direction of propagation and recovers the overall phase or wave front of the input beam in a time-reversed manner. This process is most easily accomplished by use of the photorefractive effect[7,8] in nonlinear crystals and in spectral regions (e.g., 500–1500 nm) that are commensurate with those frequently used for optical laser trapping. When a phase-conjugate beam is used as one of the beams in a double-beam trapping geometry, a laser trap can be created that combines features of both optical trapping and OPC, including specimen manipulation, tensiometric measurement, and optical image processing functions such as aberration correction,[5,6] novelty filtering,[5,9] and contrast reversal.[5,10] Such a trap should prove to be a useful tool in the fields of biology and biomedicine in which the handling, manipulation, and image processing of biological specimens are routinely performed.

In this paper we report what are to our knowledge the first experimental demonstration and theoretical study of a two-beam optical trap that uses a pair of self-aligned, mutually phase-conjugate beams. A $BaTiO_3$ crystal self-pumped by a strong Gaussian beam (~100 mW) in the CAT configuration[11] is used to phase conjugate a signal beam[12,13] transmitting through a sample cell containing latex microspheres. Both beams are derived from a cw argon laser (514.5 nm). The forward-propagating signal and counterpropagating phase-conjugate beams form a self-aligned optical trap that is stable for objective lenses with numerical apertures in the 0.40–0.85 range. For incident (signal) beam powers of ~5–~11 mW, a stable and

0740-3224/97/040697-08$10.00

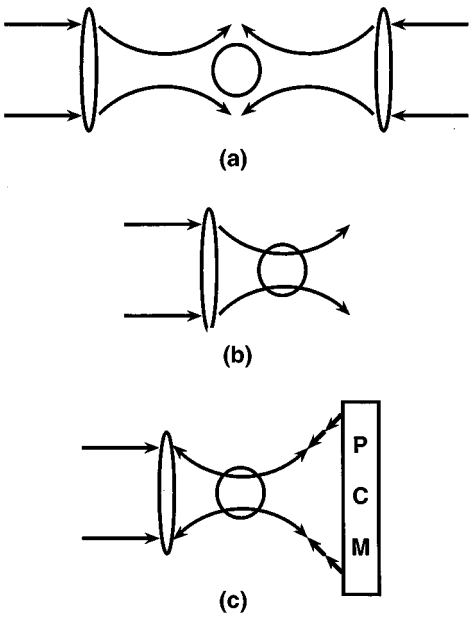

Fig. 1. Schematic showing three different optical trapping configurations: (a) counterpropagating dual-beam trap, (b) single-beam gradient force trap, and (c) mutually phase-conjugate dual-beam trap that uses a phase-conjugate mirror (PCM).

high-fidelity phase-conjugate beam with a reflectivity of nearly 400% is realized. Experimental results indicate that the transverse trapping efficiency for 2.8-μm-diameter microspheres in the two-beam phase-conjugate trap is comparable with that of a single-beam (gradient force) trap. Theoretical calculations using a ray optics model show that the two-beam phase-conjugate trap offers a slight improvement in axial trapping efficiency over that of a single-beam trap. The performance of a phase-conjugate trap is compared with that of a conventional counterpropagating dual-beam trap. Finally, the advantages and limitations of each configuration, as well as the applications of phase-conjugate trapping to biology and other fields, are discussed.

2. EXPERIMENTAL METHODS

The experimental setup used to implement phase-conjugate optical trapping is shown schematically in Fig. 2. The output from a cw argon laser (514.5 nm), operating in the TEM_{00} mode, is divided into orthogonally polarized pump (e-polarized) and signal (o-polarized) beams by a polarizing-cube beam splitter (BS_1). The beam power ratio in the two arms is adjusted by a rotating half-wave ($\lambda/2$) plate placed before the beam splitter. The signal (primary trapping) beam is first expanded and collimated by a beam expander (BE), prefocused by a 20-cm focal-length (f.l.) lens (L_1), and then focused onto a sample by a microscope objective (MO_1). Light that is scattered and transmitted through the sample is collected by a second, identical-objective lens (MO_2). The polarization of the transmitted beam is rotated by 90° by another half-wave plate and subsequently filtered by a polarizer to match that of the pump beam. Two other lenses, with focal lengths of 64 mm (L_2) and 1 m (L_3), then focus the coherent signal and pumping beams onto a $BaTiO_3$ crystal at incident angles of 49° (θ_2) and 11° (θ_1), respectively. In this configuration, the pump beam is self-pumped in the CAT configuration by means of optical feedback from total internal reflection,[11] whereas the signal beam is phase conjugated by four-wave mixing with the pump beam.[12,13] Beam splitters were used to deflect portions of the signal and the phase-conjugate beams to photodetectors D_1 and D_2, respectively, for power monitoring. The phase-conjugate beam returning from the $BaTiO_3$ crystal is collected by MO_2 and focused to exactly the same position as that of the primary trapping beam. Hence a dual-beam optical trap is created by use of counterpropagating mutually phase-conjugate beams that have near-Gaussian intensity profiles. The pump beam power was set in the range of 20–50 times the signal beam power at the entrance face of the $BaTiO_3$ crystal. The phase-conjugate reflectivity, which we obtained by taking the ratio of the powers in the conjugate and the signal beams (at D_1 and D_2), was ~400% and was very stable ($\leqslant \pm 5\%$ fluctuation).

To quantify the effects of optical trapping, we focused the mutually phase-conjugate beams onto a sample chamber containing a water suspension of 2.8-μm-diameter latex microspheres with a relative refractive index of 1.18. We estimated the optical power reaching the specimen by measuring the laser power entering the back aperture of the MO and applying a transmission correction factor for each MO.[4] All MO's have a transmittance of >70% at 514.5 nm. The phase-conjugate beam power in the trapping plane was limited to ~65–~70% of the incident beam power because the optical gain in the phase-conjugation process was not sufficient to compensate for the losses in the present configuration. To measure the transverse optical trapping efficiency we employed a viscous drag force technique.[4] An escape velocity is measured when the applied optical force is precisely balanced by the viscous drag force exerted by fluid flow. The trapping efficiency Q is determined from the expression $Q = 6\pi\eta r v c/nP$, where v is the escape velocity, r is the

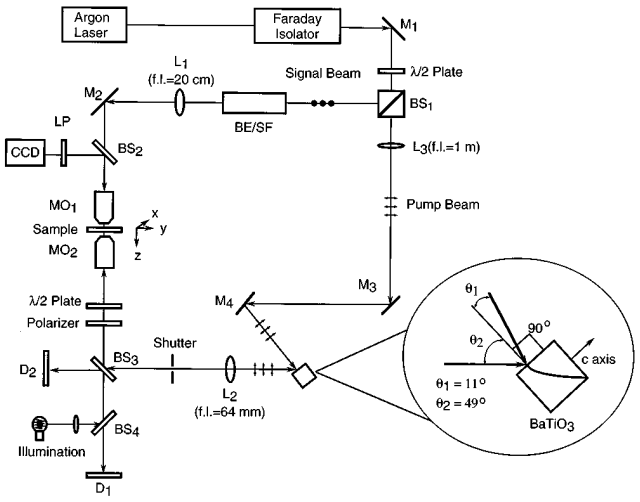

Fig. 2. Experimental system for the demonstration of optical laser trapping microscopy combined with photorefractive phase conjugation. A $BaTiO_3$ crystal is used to generate a counterpropagating phase-conjugate beam that is combined with a primary beam to form a self-aligned dual-beam trap. M's, mirrors; BS's beam splitters.

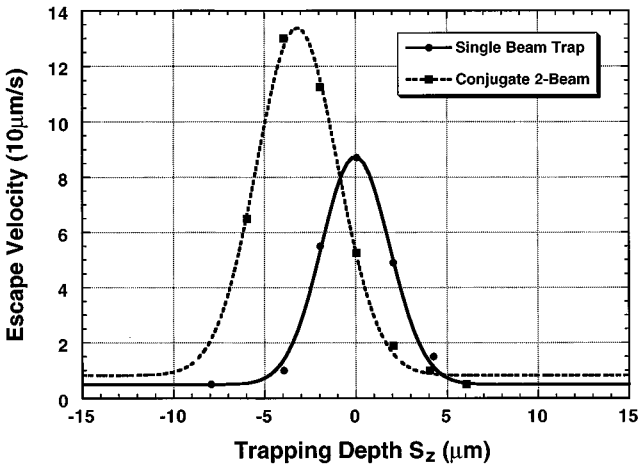

Fig. 3. Transverse escape velocity as a function of the relative axial trapping position (s_z) for a 2.8-μm-diameter polystyrene bead confined by a single beam gradient force trap (filled circles) or a self-aligned dual-beam phase-conjugate trap (filled squares) measured with a 40× (0.65-N.A.) microscope objective.

Table 1. Summary of Optical Parameters and Transverse Trapping Efficiencies for Single-Beam and Phase-Conjugate Dual-Beam Laser Traps

Microscope Objective	Incident Beam Power (mW)	Phase-Conjugate Beam Power (mW)	Q^a	
			Single Beam	Dual Beam
60× 0.85 N.A.	11.4	7.3	0.04	0.04
40× 0.65 N.A.	5.4	3.8	0.10	0.08
20× 0.40 N.A.	6.9	4.8	0.08	0.06

[a] The standard deviation for Q is ±0.01.

particle radius, η is the fluid viscosity, P is the laser power at the sample plane, n is the surrounding medium's refractive index, and c is the speed of light. For two-beam trapping the total power incident upon the trapped sample during phase conjugation is equal to the sum of optical powers in the forward-propagating signal and counterpropagating phase-conjugate beams. A motorized actuator was used to translate the chamber and provide a direct readout of escape velocity to within ±1 μm/s. A shutter was placed along the beam path to block the phase-conjugate beam during the measurement of single-beam escape velocity.

3. EXPERIMENTAL RESULTS

The results of our optical trapping experiments using the phase-conjugate geometry of Fig. 2 are presented in Fig. 3 and Table 1. Three different objectives, 60× (0.85 N.A.), 40× (0.65 N.A.), and 20× (0.40 N.A.) (Newport M series microscope objective lenses, normally used for spatial filtering) were tested in the experiments. An example of the measured transverse escape velocity as a function of the relative axial trapping position for the two trapping configurations is shown in Fig. 3 for the case of a 40× objective lens. For the same incident power of the principal trapping beam, the peak escape velocity measured for the phase-conjugate trap was found to be ~60% greater than the corresponding value of the single-beam trap. However, if one takes into account the higher power incident upon the particle in the presence of two beams versus that in a single beam, the trapping efficiency of the phase-conjugate trap is only slightly less than that of the single-beam trap. A considerable amount of signal power is lost because of scattering out of the acceptance aperture of objective MO_2. In addition, it is seen that the optimal trapping position for the phase-conjugate trap is shifted by ~3 μm toward the primary beam relative to the position where optimized single-beam trapping occurs. This behavior is expected because the equilibrium positions for the two configurations are different. In particular, the counterpropagating phase-conjugate beam contributes an additional scattering force component that opposes the scattering force from the primary signal beam, thereby resulting in an equilibrium shift.

The results of transverse trapping efficiency (Q) measurements in single- and dual-beam geometries are summarized in Table 1 for the three different MO's. For all three MO's, both gradient force and dual-beam traps could be created with only a few milliwatts (≤12 mW) of incident laser power. Whereas the measured values of Q were much smaller than the transverse efficiencies that can be achieved by MO's with much larger numerical apertures,[14] these values did not appear to change substantially over their single-beam values when the phase-conjugate beam was introduced. In addition, the highest-magnification MO with the largest N.A. (60×, 0.85 N.A.) was found to produce the lowest transverse Q. Although we do not fully understand this result, we speculate that it may be attributed to poor lens quality, aberration effects, or misalignment of the incident beam, because the transverse Q is expected to increase with increasing lens N.A..[14]

4. THEORY OF PHASE-CONJUGATE TRAPPING

To understand the process of self-aligned trapping in this new phase-conjugate trapping geometry, we calculate the axial trapping efficiency for an optical laser trap consisting of a pair of self-aligned mutually phase-conjugate counterpropagating beams. The results are compared with those of single-beam gradient force and conventional counterpropagating dual-beam laser traps. Phase-conjugate trapping is shown to provide a slight increase in axial trapping efficiency over that which can be achieved with single-beam trapping.

Ray-optics analysis provides a simplified means for describing laser trapping in terms of scattering and gradient forces.[15] For the argon-laser wavelength of 514.5 nm that was used in the experimentally demonstrated phase-conjugate optical trap described above, the radiation forces acting on microspheres greater than ~2 μm in diameter can be treated within the ray-optics regime. In the analysis, trapping efficiency can be decomposed into two parts, the transverse trapping efficiency and the axial trapping efficiency. In the transverse direction there always exists a trapping force as long as the relative refractive index is greater than 1.05.[15] And, as indicated in

Section 3 above, the transverse trapping efficiency of a phase-conjugate dual-beam trap is comparable with that of a single-beam trap. Hence the overall performance of a phase-conjugate dual-beam trap (relative to that of a single-beam trap) depends critically on the axial trapping efficiency of the dual-beam trap.

Referring to Fig. 4, we consider an optical trap in which the focus of the primary trapping beam is located along the axial direction (z axis) at distance s_z above the center of the sphere (O). The relative refractive index of the microsphere is taken to be 1.2. Two different dual-beam trapping geometries are shown in Fig. 4. Figure 4(a) is a phase-conjugate two-beam trap; every ray a_I hitting the sphere is accompanied by a phase-conjugate twin a_ϕ, which follows the trace of input ray a_I through the sphere in the reverse direction. Figure 4(b) represents a special case of a conventional counterpropagating two-beam trap (confocal dual-beam trap) in which the two counterpropagating beams are focused to the same point f in the absence of the particle. For every ray a_I hitting the sphere from one side, there is a collinear ray a_c hitting from the opposite direction. Each ray travels along its own path independently, with its propagation prescribed by the law of reflection and refraction. We calculate the total force

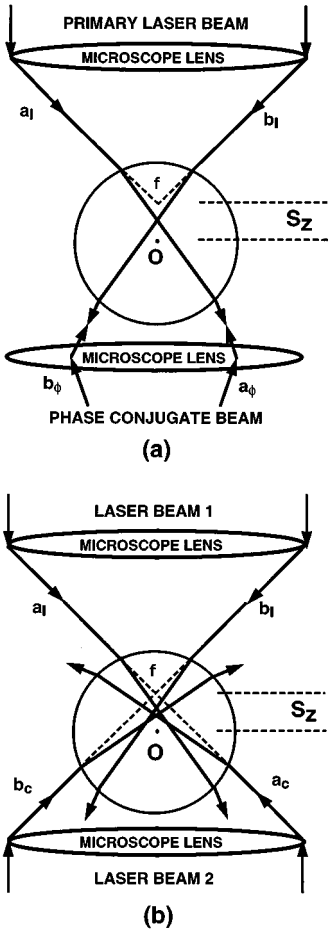

Fig. 4. Two different dual-beam trapping geometries: (a) a phase-conjugate dual-beam trap and (b) a confocal dual-beam trap. The latter is a special case of the counterpropagating dual-beam trap in which two beams are focused to the same point f in the absence of the particle.

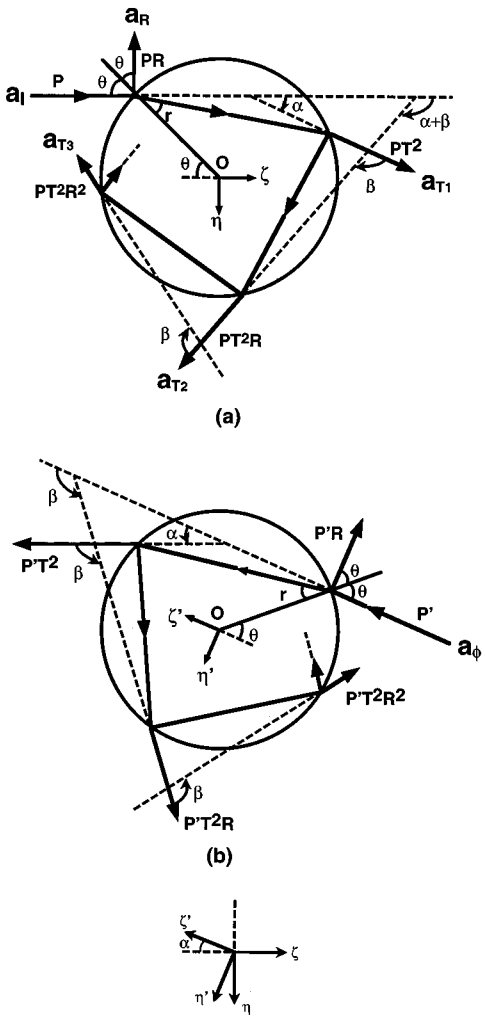

Fig. 5. Geometries for calculating the force that is due to (a) a single ray a_I of power P and (b) the phase-conjugate ray a_ϕ of power P'.

on the sphere in the two geometries by summing the contribution of each pair of rays a_I and a_ϕ or a_I and a_c entering the objective apertures and hitting the sphere.

The force that is due to a single incident ray a_I of power P hitting a dielectric sphere at an angle of incidence θ with an incident momentum per second of n_1P/c (where n_1 is the refractive index of the surrounding medium and c is the speed of light) is depicted in Fig. 5(a). In the local η–ζ coordinate system of the incident beam, the force on the sphere is given by[15]

$$F_{I_\zeta} = F_{I_s} = \frac{n_1 P}{c}\left[1 + R\cos 2\theta - \sum_{n=0}^{\infty} T^2 R^n \times \cos(\alpha + n\beta)\right]$$

$$= \frac{n_1 P}{c}\left\{1 + R\cos 2\theta - \frac{T^2[\cos(2\theta - 2r) + R\cos 2\theta]}{1 + R^2 + 2R\cos 2r}\right\}, \quad (1a)$$

$$F_{I_\eta} = F_{I_g} = \frac{n_1 P}{c}\left[0 + R\sin 2\theta - \sum_{n=0}^{\infty} T^2 R^n \times \sin(\alpha + n\beta)\right]$$

$$= \frac{n_1 P}{c}\left\{R\sin 2\theta - \frac{T^2[\sin(2\theta - 2r) + R\sin 2\theta]}{1 + R^2 + 2R\cos 2r}\right\}, \quad (1b)$$

where θ and r are the angles of incidence and refraction and T and R are the power transmittance and reflectance at the interface, respectively, and the angles α and β are shown in Fig. 5. Inasmuch as radiation forces in the geometrical-optics limit are independent of the radius (r) of the sphere, r is taken to be 1. Conventionally, the ζ component of the force is known as the scattering force (F_s), whereas the η component is known as the gradient force (F_g). The proportion of the total incident power used to exert a force on the particle, conventionally called the trapping efficiency $Q = cF/n_1P$, is given by

$$Q_{I_\zeta} = Q_{I_s} = 1 + R\cos 2\theta - \frac{T^2[\cos(2\theta - 2r) + R\cos 2\theta]}{1 + R^2 + 2R\cos 2r}, \quad (1c)$$

$$Q_{I_\eta} = Q_{I_g} = R\sin 2\theta - \frac{T^2[\sin(2\theta - 2r) + R\sin 2\theta]}{1 + R^2 + 2R\cos 2r}. \quad (1d)$$

The three terms in the force expressions [Eqs. (1a) and (1b)] are the photon momenta contributed from the incident beam (a_I), the reflected beam (a_R), and the (multiple) refracted beams (a_{T1}, a_{T2}, a_{T3}...), respectively. Numerical calculations show that contributions from the reflected beam and the multiple refraction beams account for less than 3% of the total force when the reflectance $R \ll 1$. Under such conditions, which are usually satisfied for samples such as polystyrene microspheres and biological cells, the force contribution from the first refracted beam a_{T1} ($n = 0$ term in the summation series) dominates. Theoretically, both reflected and refracted beams would be phase conjugated as long as they were collected by objective MO_2. In practice, only the first refracted beam (a_{T1}) is effectively collected by MO_2 and phase conjugated. Hence only the contribution from phase-conjugate beam of a_{T1} is considered, and less than 3% error is expected from this approximation.

The force that is due to a single phase-conjugate ray a_ϕ, which is incident upon the particle in the direction opposite that of a_{T1} with power P', is depicted in Fig. 5(b). In the local η'–ζ' coordinates of beam a_ϕ it has an expression identical to that of F_η and F_ζ [Eqs. (1)], except that P is replaced by P'. In terms of the local η–ζ coordinate system of incident beam a_I, the total force of the pair of incident beam a_I and phase-conjugate beams a_ϕ is given by

$$F_{T\phi_\zeta} = F_{T\phi_s} = F_{I_s} - \gamma(F_{I_s}\cos\alpha + F_{I_g}\sin\alpha), \quad (2a)$$

$$F_{T\phi_\eta} = F_{T\phi_g} = F_{I_g} - \gamma(F_{I_s}\sin\alpha - F_{I_g}\cos\alpha), \quad (2b)$$

where $\gamma = P'/P$ is the ratio of the power in beams a_ϕ and a_I. The corresponding trapping efficiency is

$$Q_{T\phi_s} = \frac{Q_{I_s} - \gamma(Q_{I_s}\cos\alpha + Q_{I_g}\sin\alpha)}{1 + \gamma}, \quad (2c)$$

$$Q_{T\phi_g} = \frac{Q_{I_g} - \gamma(Q_{I_s}\sin\alpha - Q_{I_g}\cos\alpha)}{1 + \gamma}, \quad (2d)$$

where the subscripts T and ϕ are used to denote the total force contribution from a pair of incident and phase-conjugate beams (a_I and a_ϕ), respectively, in a phase-conjugate configuration.

For a confocal dual-beam trap the force F_c contributed by confocal beam a_c can be expressed in terms of F_I. Taking into account the symmetry of the scattering force component and the antisymmetry of the gradient force component, we have

$$F_{c_s}(s_z) = F_{I_s}(-s_z) = F_{I_s}(s_z),$$

$$F_{c_g}(s_z) = F_{I_g}(-s_z) = -F_{I_g}(s_z).$$

It is straightforward to show that in the local η–ζ coordinate system of incident beam a_I the scattering force and the gradient force from collinear ray a_c with power P' can be expressed as $-\gamma F_{I\zeta}$ and $\gamma F_{I\eta}$, respectively, where $\gamma = P'/P$ is ratio of the power of the collinear beams. The total force from the pair of rays a_I and a_c is

$$F_{Tc_s} = (1 - \gamma)F_{I_s}, \quad (3a)$$

$$F_{Tc_g} = (1 + \gamma)F_{I_g}. \quad (3b)$$

Equations (3a) and (3b) indicate that the scattering forces from a pair of counterpropagating rays (as represented by a_I and a_c) cancel, while the corresponding gradient forces reinforce. The corresponding trapping efficiency is given by

$$Q_{Tc_s} = \frac{1 - \gamma}{1 + \gamma} Q_{I_s}, \quad (3c)$$

$$Q_{Tc_g} = Q_{I_g}, \quad (3d)$$

where the subscripts T and c are used to denote the total force contribution from a pair of collinear beams a_I and a_c in the confocal configuration.

To determine the total force along the direction of the optical axis from all the beams one needs to transform each vector from the local coordinate η–ζ system associated with a particular incident beam into the lab coordinate (x–y–z) system and integrate the z component of each contribution up to a maximum convergence angle $\phi_{\max}$ dictated by the numerical aperture of the objective lens. Such a procedure, as applied to Eqs. (1a), (2a), and (3a), yields the total scattering force along the axial direction for the cases of a single-beam trap, a phase-conjugate dual-beam trap, and a confocal two-beam trap, respectively. Likewise, the total gradient force along the axial direction for the three cases is obtained from numerical

integration of Eqs. (1b), (2b), and (3b). For each configuration the net force along the axial direction is given by the algebraic sum of scattering and gradient contributions.

5. THEORETICAL RESULTS

Theoretical results for the scattering and gradient force trapping efficiencies (Q_s and Q_g) are plotted as a function of s_z in Fig. 6 for the case of $\gamma = 1$ and $\phi_{\max} = 20°$ (corresponding to N.A. = $n_{\text{water}} \sin \phi_{\max} = 0.45$), and Fig. 7 compares the total trapping efficiency (Q_t) for two different beam convergence angles ($\phi = 20°, 60°$). Figure 6(a) reveals the differences in the net scattering force (and the scattering efficiency) along the axial direction for the three configurations in which the distance s_z is dimensionless (i.e., normalized to the radius of the sphere, r). In a single-beam trap the scattering force along the axial direction pushes the particle downstream away from the incoming beam. Hence the sign of Q_s in Fig. 6(a) is always positive. The gradient force, on the other hand, is negative for $s_z > 0$ and positive for $s_z < 0$. It acts as a spring that provides a restoring force. In general, the gradient efficiency is nearly the same for all three cases [Fig. 6(b)]. In the confocal two-beam geometry the scattering force from each of the counterpropagating pair of rays exactly cancels the other along the axial direction in the special case of $\gamma = 1$. Consequently the net scattering force along the axial direction always vanishes, regardless of the value of s_z. In contrast, complete cancellation occurs only at $s_z = 0$ for the phase-conjugate dual-beam geometry when the phase-conjugate beam and the primary incoming beam are symmetrically counterpropagating with respect to $s_z = 0$. At any other positions, both scattering and gradient force components are reinforced by the phase-conjugate beam because the phase-conjugate beam retraces the path of the original beam. However, the gradient force is reinforced more than the scattering force. Hence there is some improvement in the trapping efficiency in the phase-conjugate dual-beam trap compared with that of a single-beam trap.

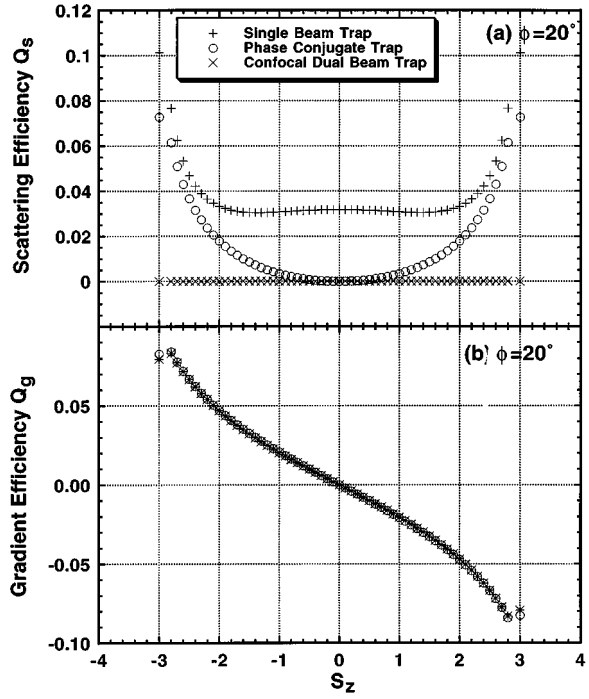

Fig. 6. Comparison of (a) scattering efficiency (Q_s) and (b) gradient efficiency (Q_g) for a single-beam gradient force trap, a phase-conjugate dual-beam trap, and a confocal dual-beam trap. The maximum convergence angle is taken to be $\phi_{\max} = 20°$. Refractive indices of $n_1 = 1.33$ (water) and $n_2 = 1.59$ (latex microsphere), and a relative refractive index $n = 1.2$ have been used. The microsphere radius is taken to be 1.

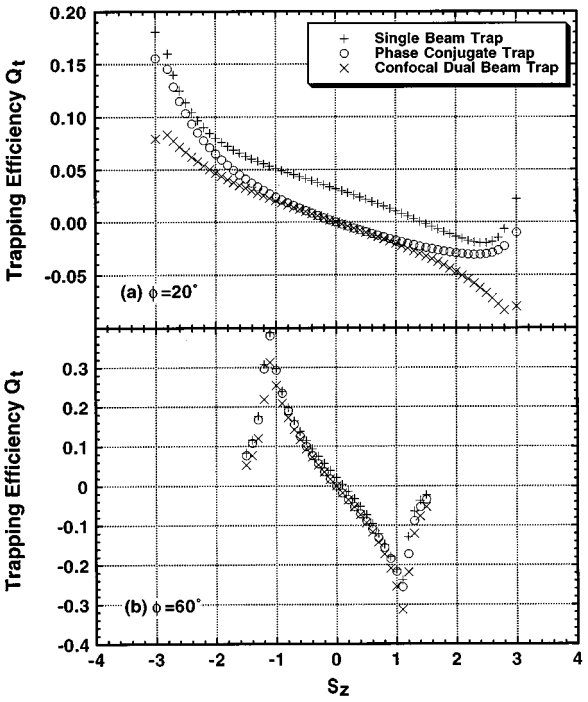

Fig. 7. Comparison of the total trapping efficiency (Q_t) for the three trap configurations when the relative refractive index is $n = 1.2$ and (a) $\phi_{\max} = 20°$, (b) $\phi_{\max} = 60°$.

The regions of stable trapping and the corresponding equilibrium positions also differ in the three configurations. Figure 7(a) shows that the trapping zone of a confocal two-beam trap extends farthest in the $s_z > 0$ region, followed by the phase-conjugate trap and then the single-beam trap. The significance of this advantage, however, decreases as the numerical aperture of the objective lens increases, as illustrated in Fig. 7(b) for the case of $\gamma = 1$ and $\phi_{\max} = 60°$ (N.A. 1.15) where the gradient force dominates the scattering force. A comparison of axial trapping efficiency for different values of beam power ratio γ is plotted in Fig. 8(a), which shows that the axial trapping efficiency of a phase-conjugate trap is less sensitive to the variation in γ than that of the confocal two-beam trap. In general, two counterpropagating beams need not be confocal. The dependence of axial trapping efficiency on s_z for different values of separation ($d > 0$ for the far-field region) between the foci of the two beams is plotted in Fig. 8(b). These results show that the advantage of a two-beam trap over a single-beam trap degrades rapidly as one moves to the far-field region.

6. DISCUSSION

An optical laser trap based on the OPC process has several unique features that make it suitable for sample micromanipulation and optical image processing. First, by virtue of the fact that a phase-conjugate beam precisely reverses its direction and recovers its phase along the original propagation path, the signal and the conjugate trapping beams are intrinsically self-aligned and are brought to focus at the same spatial position where a trap is to be formed. This eliminates the need to align counterpropagating beams critically to within the dimensions of a beam waist. Second, by optimizing the orientation of the pump and the signal beams with respect to the $BaTiO_3$ crystal it is possible to achieve a large photorefractive gain (in phase conjugation) that is stable over a broad range of pump and signal beam powers. With sufficient gain, dual-beam optical trapping can be implemented for smaller primary signal beam powers. In addition, trapping can be performed with lower-N.A. objective lenses. Finally, by combining optical trapping with photorefractive phase conjugation it should be possible to implement many of the nonlinear-optical signal processing functions that are unique to OPC, including aberration correction of phase objects,[5,8] contrast reversal,[8,10] and transient detection of moving objects.[8,9]

The key advantage of a single-beam gradient trap is its simplicity. For objective lenses with sufficiently large N.A. (N.A. $\geqslant$ 0.85) a single-beam trap provides very good axial and transverse trapping efficiencies ($Q \sim 0.1$–0.3).[14] Although optical trapping using two counterpropagating beams can offer higher axial trapping efficiency, critical alignment of the two beams to within a fraction of a wavelength is required. As one moves into the far-field region the trapping efficiency for a conventional dual-beam trap degrades rapidly to a point beyond which the two-beam trap ceases to function unless other approaches such as alternating light beams[16] are used. The phase-conjugate two-beam trap eliminates the alignment requirement, can be implemented with lower-N.A. objectives, and, under certain conditions, gives slight improvement in the axial trapping efficiency over the single-beam trap, as shown in Figs. 6 and 7. The experimental results of Fig. 3 and Table 1 also indicate that relatively strong transverse optical confinement effects can be obtained, even for a 40 × 0.65-N.A. lens. The larger Rayleigh range and depth of focus of lower-N.A. lenses might, therefore, facilitate stable trapping over a broader range of axial positions than is possible with higher-N.A. (e.g., 100× 1.3-N.A.) objectives.

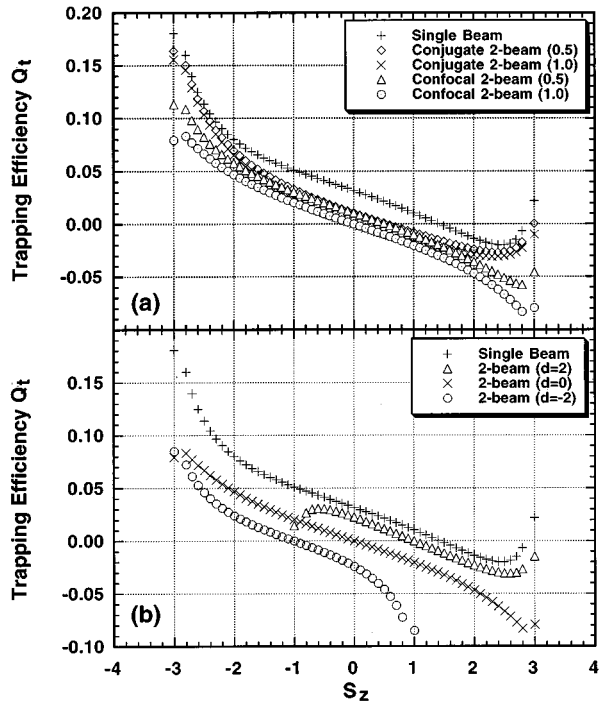

Fig. 8. (a) Comparison of trapping efficiency (Q_t) for single-beam, phase-conjugate beam, and confocal dual-beam traps for different values of beam power ratio $\gamma = P'/P$ with $\phi_{max} = 20°$ and $n = 1.2$. (b) Comparison of Q_t values for a counterpropagating dual-beam trap for different separations d between the foci of the two beams ($d > 0$ in far-field region) with $\phi_{max} = 20°$ and $n = 1.2$.

Though it is nontrivial to achieve a stable phase-conjugate beam with high phase-conjugate reflectivity ($R_\phi \gg 1$), there are several features of phase conjugation, as it relates to optical image processing, that make it attractive for use in various biological applications in which optical tweezers have been extensively used for sample confinement and micromanipulation.[4] For example, a phase-conjugate trap might find use in the correction of aberrations and the enhancement of image contrast during the confinement and manipulation of cells, organelles, and other cellular substructures that are embedded in phase aberrative media within cell and tissue samples. By conjugating the trap (signal) beam back through the biological sample, it might be possible to correct for the aberrations and phase distortions introduced by the surrounding medium or the sample itself. The most interesting applications lie in the unique novelty filtering (transient detection) feature of OPC, which renders moving objects visible and all stationary objects invisible, as demonstrated by Chiou *et al.*[5] It may be used to study cytoskeleton muscle fiber motions triggered by biochemical cascades or the dynamics of chromosome movement during cell mitosis. Motility of a sperm could be studied with its head trapped and the motion of the tail be monitored by phase-conjugation imaging. It has been of great interest in studying the motion of a protozoan impelled by external chemical or biological stimulus. However, the detection of the motion is sometimes hindered because of the existence of disturbing background in imaging. Optical trapping combined with phase-conjugation imaging may provide a better alternative to these studies.

If such applications of phase-conjugate trapping are to be realized, several issues need to be addressed in more detail. These include (1) the choice of a suitable laser wavelength (preferably near-infrared) that would facilitate both efficient phase conjugation and minimization of absorption effects by important biological chromophores; (2) the study of photorefractive crystals that would optimize the photorefractive response time, especially for transient detection applications; and (3) the study of the types of biological specimen that can serve as good phase objects, be efficiently trapped, and provide interesting image processing challenges. Using this novel laser trap-

ping geometry, we are investigating these and other issues and applications.

7. SUMMARY

In summary, we have described what are to our knowledge the first experimental demonstration and theoretical analysis of a self-aligned dual-beam optical laser trap based on optical phase conjugation. The trap has the unique features of being self-aligned, using relatively small-numerical-aperture objective lenses, achieving a small enhancement in axial trapping efficiency, and providing a capability for the implementation of nonlinear-optical signal processing functions. Thus the self-aligned phase-conjugate laser trap should find applications in fields that require the confinement and image analysis of dielectric and biological samples on a microscopic scale.

ACKNOWLEDGMENTS

This research was supported by grants from the National Science Foundation (ECS-9413956) and the National Institutes of Health (5P41-RR01192-15). The authors thank A. Harvey for his support and encouragement and Y. Liu for helpful discussions.

REFERENCES

1. A. Ashkin, "Acceleration and trapping of particles by radiation pressure," Phys. Rev. Lett. **24**, 156–159 (1970).
2. A. Ashkin, J. M. Dziedzic, J. E. Bjorkholm, and S. Chu, "Observation of a single-beam gradient force optical trap for dielectric particles," Opt. Lett. **11**, 288–290 (1986).
3. A. Ashkin and J. M. Dziedzic, "Optical trapping and manipulation of viruses and bacteria," Science **235**, 1517–1520 (1987).
4. K. Svoboda and S. M. Block, "Biological applications of optical forces," Annu. Rev. Biomol. Struct. **23**, 247–285 (1994).
5. A. E. Chiou, J. Hong, G. J. Sonek, Y. Liu, and M. W. Berns, "Image processing and trapping of microscopic objects using a phase conjugate Michelson interferometer," in *Biomedical Fiber Optic Instrumentation,* J. A. Harrington, D. M. Harris, A. Katair, and F. P. Milanovich, eds., Proc. SPIE **2131**, 406–416 (1994).
6. R. A. Fisher, ed., *Optical Phase Conjugation* (Academic, New York, 1983).
7. P. Gunter and J.-P. Huignard, in *Photorefractive Materials and Their Applications I: Fundamental Phenomena*, P. Gunter and J.-P. Huignard, eds. (Springer-Verlag, Berlin, 1988), pp. 7–23.
8. P. Yeh, *Introduction to Photorefractive Nonlinear Optics* (Wiley, New York, 1993).
9. R. S. Cudney, R. M. Pierce, and J. Feinberg, "The transient detection microscope," Nature (London) **332**, 424–426 (1988).
10. A. E. Chiou, P. Yeh, and M. Khoshnevisan, "Nonlinear optical image subtraction for potential industrial applications," Opt. Eng. **27**, 385–392 (1988).
11. J. Feinberg, "Self-pumped, continuous-wave phase conjugator using internal reflection," Opt. Lett. **7**, 486–488 (1982).
12. A. Chiou, T. Y. Chang, and M. Khoshnevisan, "High-speed photorefractive phase conjugator with large dynamic range and wide field of view," in *OSA Annual Meeting*, Vol. 15 of 1990 OSA Technical Digest Series (Optical Society of America, Washington, D.C., 1990), p. 40.
13. P. Yeh and A. Chiou, in *Real-Time Optical Information Processing*, B. Javidi and J. L. Horner, eds. (Academic, Boston, Mass., 1994).
14. W. H. Wright, G. J. Sonek, and M. W. Berns, "Parametric study of the forces on microspheres held by optical tweezers," Appl. Opt. **33**, 1735–1748 (1994).
15. A. Ashkin, "Forces of a single-beam gradient laser trap on a dielectric sphere in the ray optics regime," Biophys. J. **61**, 569–582 (1992).
16. A. Ashkin and J. M. Dziedzic, "Observation of radiation-pressure trapping of particles by alternating light beams," Phys. Rev. Lett. **54**, 1245–1248 (1985).